

Jeffrey Fluid Performance on MHD Convective Flow Past a Semi-Infinite Vertically Inclined Permeable Moving Plate in Presence of Heat and Mass Transfer: a Finite Difference Technique

Y.Sunita Rani*

*Research Scholar, Department of Mathematics
Rayalaseema university, Kurnool, Pin:518007, Andhra Pradesh State, India.*

**Corresponding author*

M.V.Ramana Murthy

*Department of Mathematics & Computer sciences,
University College of Science, Osmania University, Hyderabad, India.*

G.Vani Sree

*Department of Mathematics, Arjun College of Technology & Sciences
Batasingaram, R.R. Dist, Hyderabad, India.*

G. Kamala

*Department of mathematics & computer sciences, University College for
sciences, Osmania University, Hyderabad-500007, Telanagana State, India.*

Abstract

This paper is concerned with the study of an unsteady, MHD natural convective boundary layer flow of a viscous, incompressible and electrically conducting, non-newtonian Jeffrey fluid over a semi-infinite vertically inclined permeable moving plate embedded in a porous medium in the presence of heat absorption, heat and mass transfer. The fundamental governing equations for this investigation are solved numerically using the finite difference technique. Numerical evaluation of the numerical results is performed and graphical results for the velocity, temperature and

concentration profiles within the boundary layer are presented graphically and discussed. Also, the expressions for the skin-friction coefficient, rate of heat and mass transfer coefficients have been derived and plotted for different values of the governing parameters. The obtained numerical results reduce to previously published results on a special case of the problem.

Keywords: Jeffrey fluid; MHD; Natural Convection flow; Heat and Mass transfer; Finite difference method;

NOMENCLATURE:

List of Variables:

- x', y' Co-ordinate system (m)
- O Origin
- B_o Magnetic field component along y' – axis (*Tesla*)
- C_p Specific heat at constant pressure ($J-K/Kg$)
- g Acceleration of gravity, $9.81 (m/s^2)$
- D Chemical molecular diffusivity ($m^2 s^{-1}$)
- C' Concentration of fluid near the plate ($mol m^{-3}$)
- M Hartmann number
- S Heat absorption parameter
- Nu Nusselt number (or) Rate of heat transfer
- U_p Plate Velocity (m/s)
- Pr Prandtl number
- Gc Grashof number for mass transfer
- C'_∞ Concentration of the fluid at infinity ($mol m^{-3}$)
- x, y Dimensionless coordinates (m)
- u, v Components of velocities along and perpendicular to the plate respectively, x' – direction (m/s)
- Q_o Dimensional Heat absorption parameter
- U_o Reference velocity (m/s)
- R_{e_x} Reynold's number
- u', v' Non-dimensional components of velocities along and perpendicular to the plate respectively, x' – direction (m/s)
- Gr Grashof number for heat transfer

C'_w	Concentration of the fluid far away of the fluid from the plate ($mol\ m^{-3}$)
t'	Dimensional time (<i>second</i>)
Sc	Schmidt number
Sh	Sherwood number (or) Rate of mass transfer
V_o	Suction velocity (m/s)
U_∞	Free stream velocity (m/s)
u'_p	Dimensional Plate Velocity (m/s)
n'	Dimensional exponential index
n	An exponential index
K'	The permeability of medium (m^2)
T'	Temperature of fluid near the plate (K)
T'_∞	Temperature of the fluid at infinity (K)
T'_w	Temperature of the fluid far away of the fluid from the plate (K)
u'	Velocity component in x' – direction (m/s)
K	The permeability parameter (m^2)
t	Time (<i>second</i>)
y	Dimensionless coordinate (m)

Greek symbols

β	Coefficient of volume expansion for heat transfer (K^{-1})
β^*	Coefficient of volume expansion for mass transfer ($m^3\ Kg^{-1}$)
ϕ	Concentration of the fluid ($mol\ m^{-3}$)
ρ	Density of the fluid (kg/m^{-3})
σ	Electrical conductivity of the fluid ($\Omega^{-1}m^{-1}$)
ν	Kinematic viscosity (m^2s^{-1})
θ	Non-dimensional temperature (K)
nt	Phase angle (<i>degrees</i>)
τ	Skin-friction (N/m^2)
κ	Thermal conductivity of the fluid (W/mK)
α	Angle of inclination (<i>degrees</i>)
λ	Jeffrey fluid parameter
ε	A positive constant

Superscripts

' Dimensionless properties

Subscripts

p Plate

w Wall condition

∞ Free stream condition

1. INTRODUCTION:

MHD is the science of motion of electrically conducting fluids in presence of magnetic field. It concerns with the interaction of magnetic field with the fluid velocity of electrically conducting fluid. MHD generators, MHD pumps and MHD flow meters are some of the numerous examples of MHD principles. Dynamo and motor are classical examples of MHD principle. Convection problems of electrically conducting fluid in presence of magnetic field have got much importance because of its wide applications in Geophysics, Astrophysics, Plasma Physics, Missile technology, etc. MHD principles also find its applications in Medicine and Biology. Magnetohydrodynamics has many industrial applications such as physics, chemistry and engineering, crystal growth, metal casting and liquid metal cooling blankets for fusion reactors. The convective heat transfer over a stretching surface with applied magnetic field was presented by Vajravelu et al. [1]. Pop and Na [2] studied the influence of magnetic field flow over a stretching permeable surface. Xu et al. [3] presented a series solutions of the unsteady three-dimensional MHD flow and heat transfer over an impulsively stretching plate. Nazar et al. [4] analyzed the hydro magnetic flow and heat transfer over a vertically stretched sheet and found that an increase in the magnetic parameter local skin friction and heat flux at the wall decreases. The effect of MHD stagnation point flow towards a stretching sheet was investigated by Ishak et al. [5]. Kiran Kumar et al. [6] and [7] analyzed the study of heat and mass transfer enhancement in free convection flow with chemical reaction and thermo-diffusion in nanofluids through porous medium in a rotating frame. Venkateswarlu and Satyanarayana [8] have studied the effects of chemical reaction and radiation absorption on the heat and mass transfer flow of nanofluid in a rotating system. Some of them are Mansour [9], Ganesan and Loganathan [10], Mbeledogu et al. [11], Makinde [12], Samad and Rahman [13], Orhan and Ahmet [14], Prasad et al. [15], Takhar et al. [16], Gebhart et al. [17], Ali et al. [18], Hossain et al. [19], Hossain et al. [20], Ghaly [21], Muthucumaraswamy and Janakiraman [22], Muthucumaraswamy and Sivakumar [23], Ahmed and Dutta [24], Ahmed [25], Muthucumaraswamy et al. [26], Chamkha [27], Srinivasa Raju [28], Srinivasa Raju et

al. [29], Srinivasa Raju et al. [30], Srinivasa Raju et al. [31], Srinivasa Raju et al. [32], Srinivasa Raju [33], Jithender Reddy et al. [34].

The present objective is to attempt a mathematical model of heat and mass transfer in Jeffrey fluid flow over a permeable moving plate with heat and mass transfer in the presence of applied magnetic field and heat absorption. The study has importance in many metallurgical processes including magma flows, polymer and food processing, and blood flow in micro-circulatory system etc. Similarity variables are employed to convert the non-linear coupled partial differential equations into linear coupled partial differential equations. The transformed linear partial differential equations are solved numerically using finite difference technique. Graphs for various pertinent parameters on the velocity, temperature and concentration profiles are presented and analyzed in detail. The numerical values of friction factor, local Nusselt and Sherwood numbers are tabulated and examined. Also, a comparison of current study to the previous ones is provided to validate our solutions.

2. MATHEMATICAL FORMULATION:

The effect of heat and mass transfer on an unsteady free convective, incompressible, viscous, electrically conducting Jeffrey fluid flow past a semi-infinite vertically inclined permeable moving plate embedded in a uniform porous medium and subjected to a uniform transverse magnetic field is studied. The physical model and the coordinate system are shown in Fig. 1. For this study, In cartesian coordinate system, let x' – axis is taken to be along the plate and the y' – axis normal to the plate. Since the plate is considered infinite in x' – direction, hence all physical quantities will be independent of x' – direction. A uniform magnetic field of magnitude B_0 is applied normal to the plate. The transverse applied magnetic field and magnetic Reynold's number are assumed to be very small, so that the induced magnetic field is negligible. The wall is maintained at constant temperature (T'_w) and concentration (C'_w) higher than the ambient temperature (T'_∞) and concentration (C'_∞) respectively. The fluid properties are assumed to be constant except that the influence of density variation with temperature has been considered only in the body-force term. The fluid has constant kinematic viscosity and constant thermal conductivity, and the Boussinesq's approximation have been adopted for the flow. At time $t' > 0$ the plate is given an impulsive motion in the direction of flow i.e. along x' – axis against the gravity with constant velocity U_p . It is assumed that there is no applied voltage which implies the absence of an electric field. In addition, it is assumed that the temperature and the concentration at the wall as well as the suction velocity are exponentially varying with time.

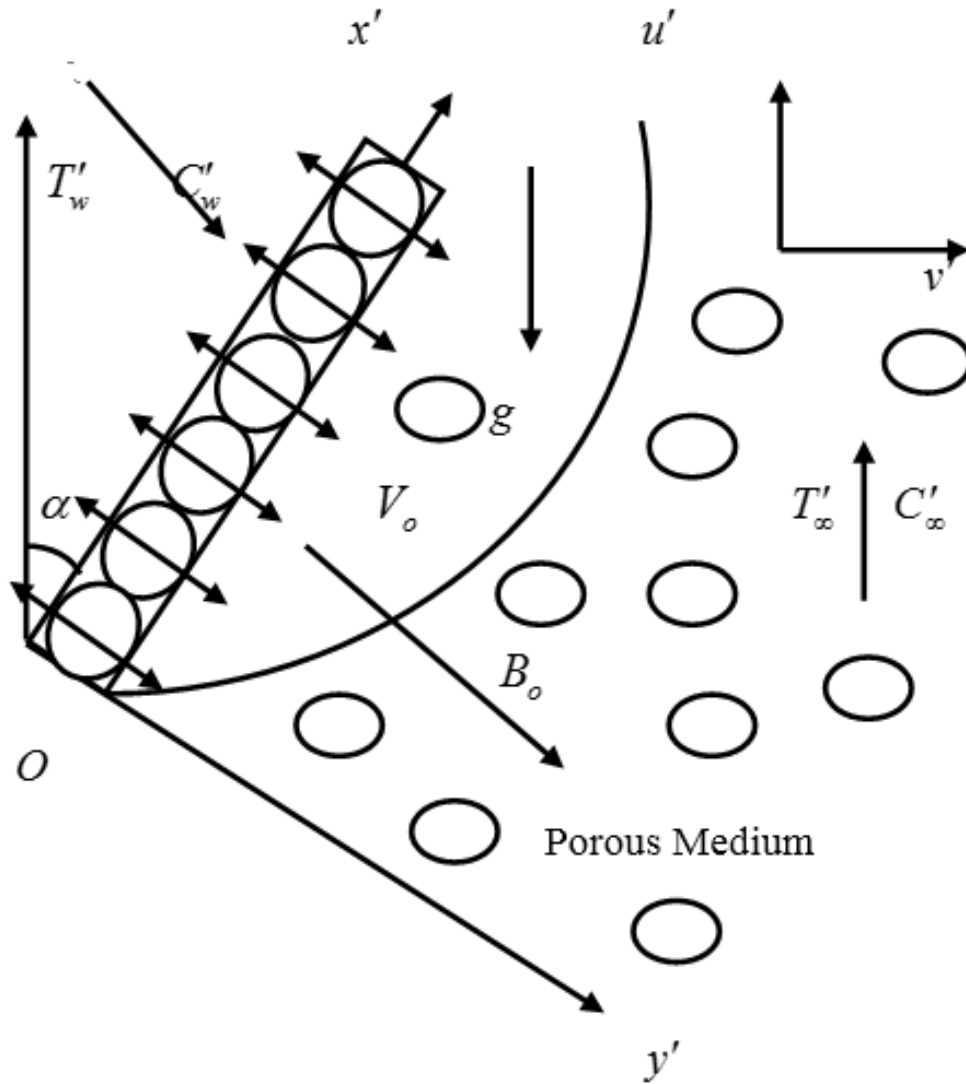


Fig. 1. Physical configuration and coordinates system

The Cauchy stress tensor, \bar{S} , of a Jeffrey's non-Newtonian fluid [35] takes the form as follows:

$$S = \frac{\mu}{1 + \lambda} \left(\dot{\gamma} + \lambda_1 \ddot{\gamma} \right) \tag{1}$$

where μ is the dynamic viscosity, λ_1 is the ratio of relaxation to retardation times, dot above a quantity denotes the material time derivative and γ is the shear rate. The Jeffrey's model provides an elegant formulation for simulating retardation and relaxation effects arising in non-Newtonian polymer flows. The shear rate and

gradient of shear rate are further defined in terms of velocity vector, \bar{V} , as follows:

where $\dot{\gamma} = \nabla \bar{V} + (\nabla \bar{V})^T$ (2)

and $\ddot{\gamma} = \frac{d}{dt}(\dot{\gamma}) + (\bar{V} \cdot \nabla) \dot{\gamma}$ (3)

Under these assumptions, the equations that describe the physical situation are given by (Chamkha [27]):

Equation of Continuity:

$$\frac{\partial v'}{\partial y'} = 0 \tag{4}$$

Momentum Equation:

$$\begin{aligned} \frac{\partial u'}{\partial t'} + v' \frac{\partial u'}{\partial y'} = & -\frac{1}{\rho} \left(\frac{\partial p'}{\partial x'} \right) + \left(\frac{v}{1+\lambda} \right) \frac{\partial^2 u'}{\partial y'^2} - \left[\frac{\sigma B_o^2}{\rho} \right] u' - \left[\frac{v}{K'} \right] u' + g\beta(T' - T'_\infty)(\cos \alpha) \\ & + g\beta^* (C' - C'_\infty)(\cos \alpha) \end{aligned} \tag{5}$$

Energy Equation:

$$\frac{\partial T'}{\partial t'} + v' \frac{\partial T'}{\partial y'} = \frac{1}{\rho C_p} \left[\kappa \frac{\partial^2 T'}{\partial y'^2} \right] - \frac{1}{\rho C_p} [Q_o (T' - T'_\infty)] \tag{6}$$

Species Diffusion Equation:

$$\frac{\partial C'}{\partial t'} + v' \frac{\partial C'}{\partial y'} = D \frac{\partial^2 C'}{\partial y'^2} \tag{7}$$

It is assumed that the permeable plate moves with a constant velocity in the direction of fluid flow and the free stream velocity follows the exponentially increasing small perturbation law. The corresponding initial and boundary conditions are

$$\left. \begin{aligned} t' \leq 0 : & u' = 0, T' = T'_\infty, C' = C'_\infty \text{ for all } y' \\ t' > 0 : & \left\{ \begin{aligned} u' = u'_p, T' = T'_\infty + \varepsilon(T'_w - T'_\infty)e^{n't'}, C' = C'_\infty + \varepsilon(C'_w - C'_\infty)e^{n't'} \text{ at } y' = 0 \\ u' \rightarrow U'_\infty = U_o(1 + \varepsilon e^{n't'}), T' \rightarrow 0, C' \rightarrow 0 \text{ as } y' \rightarrow \infty \end{aligned} \right\} \end{aligned} \right\} \tag{8}$$

From Eq. (4), it is clear that the suction velocity at the plate is either a constant or a function of time. Hence the suction velocity normal to the plate is assumed in the form

$$v' = -V_o(1 + \varepsilon A e^{n't'}) \tag{9}$$

Where A is a real positive constant, ε is a positive constant and εA is small values

less than unity, and V_o is scale of suction velocity which is non-zero positive constant. The negative sign indicates that the suction is towards the plate. Outside the boundary layer, Eq. (5) gives

$$-\frac{1}{\rho} \left(\frac{\partial p'}{\partial x'} \right) = \frac{dU'_\infty}{dt'} + \left[\frac{v}{K'} \right] U'_\infty + \frac{\sigma}{\rho} B_o^2 U'_\infty \quad (10)$$

In order to write the governing equations and the boundary conditions in dimensionless form, the following non-dimensional quantities are introduced.

$$\left. \begin{aligned} y = \frac{y'V_o}{v}, t = \frac{t'V_o^2}{v}, u = \frac{u'}{U_o}, v = \frac{v'}{V_o^2}, \theta = \frac{T' - T'_\infty}{T'_w - T'_\infty}, \phi = \frac{C' - C'_\infty}{C'_w - C'_\infty}, n = \frac{n'v}{V_o^2}, U_p = \frac{u'_p}{U_o}, M = \left(\frac{\sigma B_o^2}{\rho} \right) \frac{v}{V_o^2}, \\ Gr = \frac{g\beta v(T'_w - T'_\infty)}{U_o V_o^2}, Gc = \frac{g\beta^* v(C'_w - C'_\infty)}{U_o V_o^2}, Pr = \frac{\nu \rho C_p}{\kappa}, Sc = \frac{\nu}{D}, K = \frac{K'V_o^2}{v^2}, S = \frac{\nu Q_o}{\rho C_p V_o^2}, U_\infty = \frac{U'_\infty}{U_o} \end{aligned} \right\} \quad (11)$$

In view of Eqs (9), (10) and (11), Eqs (5) to (7) reduce to the following dimensional form:

$$\frac{\partial u}{\partial t} - (1 + \varepsilon A e^{nt}) \frac{\partial u}{\partial y} = \frac{dU_\infty}{dt} + \left(\frac{1}{1 + \lambda} \right) \frac{\partial^2 u}{\partial y^2} + (Gr)(\cos \alpha)\theta + (Gc)(\cos \alpha)\phi + N(U_\infty - u) \quad (12)$$

$$\frac{\partial \theta}{\partial t} - (1 + \varepsilon A e^{nt}) \frac{\partial \theta}{\partial y} = \frac{1}{Pr} \frac{\partial^2 \theta}{\partial y^2} - S\theta \quad (13)$$

$$\frac{\partial \phi}{\partial t} - (1 + \varepsilon A e^{nt}) \frac{\partial \phi}{\partial y} = \frac{1}{Sc} \frac{\partial^2 \phi}{\partial y^2} \quad (14)$$

Where $N = M + \frac{1}{K}$. The corresponding initial and boundary conditions in dimensionless form are:

$$\left. \begin{aligned} t \leq 0: u = 0, \theta = 0, \phi = 0 \text{ for all } y \\ t > 0: \left\{ \begin{aligned} u = U_p, \theta = 1 + \varepsilon e^{nt}, \phi = 1 + \varepsilon e^{nt} \text{ at } y = 0 \\ u \rightarrow U_\infty = 1 + \varepsilon e^{nt}, \theta \rightarrow 0, \phi \rightarrow 0 \text{ as } y \rightarrow \infty \end{aligned} \right\} \end{aligned} \right\} \quad (15)$$

For practical design purposes in MHD energy systems a number of engineering parameters provide important descriptions of the wall transport processes. The skin-friction at the plate can be obtained in non-dimensional form is given by

$$\tau = \frac{\tau'_w}{\rho U_o V_o} = \left[\frac{\partial u}{\partial y} \right]_{y=0} \quad (16)$$

The rate of heat transfer coefficient in the non-dimensional form, in terms of the Nusselt number, is given by

$$Nu = - \left[\frac{x'}{(T'_w - T'_\infty)} \frac{\partial T'}{\partial y'} \right]_{y'=0} \Rightarrow Nu(\text{Re}_x^{-1}) = \left[\frac{\partial \theta}{\partial y} \right]_{y=0} \tag{17}$$

The rate of mass transfer coefficient in the non-dimensional form, in terms of the Sherwood number, is given by

$$Sh = - \left[\frac{x'}{(C'_w - C'_\infty)} \frac{\partial C'}{\partial y'} \right]_{y'=0} \Rightarrow Sh(\text{Re}_x^{-1}) = \left[\frac{\partial \phi}{\partial y} \right]_{y=0} \tag{18}$$

Where $\text{Re}_x = - \frac{V_o x'}{\nu}$ is the Reynold's number.

3. NUMERICAL SOLUTION BY FINITE DIFFERENCE METHOD:

The non-linear momentum, energy and concentration equations given in equations (12), (13) and (14) are solved under the appropriate initial and boundary conditions (15) by the implicit finite difference method. The transport equations (12), (13) and (14) at the grid point (i, j) are expressed in difference form using Taylor's expansion.

$$\left(\frac{u_i^{j+1} - u_i^j}{\Delta t} \right) - (1 + \varepsilon A e^{nt}) \left(\frac{u_{i+1}^j - u_i^j}{\Delta y} \right) = \frac{dU_\infty}{dt} + \left(\frac{1}{1 + \lambda} \right) \left(\frac{u_{i+1}^j - 2u_i^j + u_{i-1}^j}{(\Delta y)^2} \right) + (Gr)(\cos \alpha)\theta_i^j + (Gc)(\cos \alpha)\phi_i^j + N(U_\infty - u_i^j) \tag{19}$$

$$(\text{Pr}) \left(\frac{\theta_i^{j+1} - \theta_i^j}{\Delta t} \right) - (1 + \varepsilon A e^{nt}) (\text{Pr}) \left(\frac{\theta_{i+1}^j - \theta_i^j}{\Delta y} \right) = \left(\frac{\theta_{i+1}^j - 2\theta_i^j + \theta_{i-1}^j}{(\Delta y)^2} \right) - (\text{Pr}) S \theta_i^j \tag{20}$$

$$(\text{Sc}) \left(\frac{\phi_i^{j+1} - \phi_i^j}{\Delta t} \right) - (1 + \varepsilon A e^{nt}) (\text{Sc}) \left(\frac{\phi_{i+1}^j - \phi_i^j}{\Delta y} \right) = \left(\frac{\phi_{i+1}^j - 2\phi_i^j + \phi_{i-1}^j}{(\Delta y)^2} \right) \tag{21}$$

Where the indices i and j refer to y and t respectively. The initial and boundary conditions (15) yield.

$$\left. \begin{aligned} u_i^0 &= 0, \theta_i^0 = 0, \phi_i^0 = 0 \text{ for all } i, \\ u_i^j &= U_p, \theta_i^j = 1 + \varepsilon e^{nj}, \phi_i^j = 1 + \varepsilon e^{nj} \text{ at } i = 0 \\ u_M^j &\rightarrow 0, \theta_M^j \rightarrow 0, \phi_M^j \rightarrow 0 \end{aligned} \right\} \tag{22}$$

Thus the values of u , θ and ϕ at grid point $t = 0$ are known; hence the temperature field has been solved at time $t_{i+1} = t_i + \Delta t$ using the known values of the previous

time $t = t_i$ for all $i = 1, 2, \dots, N-1$. Then the velocity field is evaluated using the already known value of temperature and concentration fields obtained at $t_{i+1} = t_i + \Delta t$. These processes are repeated till the required solution of u , θ and ϕ is gained at convergence criteria.

$$abs|(u, \theta, \phi)_{exact} - (u, \theta, \phi)_{numerical}| < 10^{-3} \quad (23)$$

4. CODE VALIDATION OF PROGRAMME:

Table-1: Comparison of present skin-friction results with the skin-friction results of Chamkha [27] for different values of Grashof number for mass transfer, Heat absorption and Schmidt number

Gc	Present skin-friction results	Skin-friction results of Chamkha [27]	ϕ	Present skin-friction results	Skin-friction results of Chamkha [27]	Sc	Present skin-friction results	Skin-friction results of Chamkha [27]
0.0	2.71896245	2.7200	0.0	3.45862241	3.4595	0.16	3.43251604	3.4328
1.0	3.27658424	3.2772	1.0	3.27658424	3.2772	0.60	3.27658424	3.2772
2.0	3.83501624	3.8343	2.0	3.19324628	3.1933	1.00	3.18462398	3.1847
3.0	4.39214668	4.3915	3.0	3.13791632	3.1378	2.00	3.04781362	3.0481

Table-2: Comparison of present Nusselt number results with the Nusselt number results of Chamkha [27] for different values of Grashof number for mass transfer, Heat absorption and Schmidt number

Gc	Present Nusselt number results	Nusselt number results of Chamkha [27]	ϕ	Present Nusselt number results	Nusselt number results of Chamkha [27]	Sc	Present Nusselt number results	Nusselt number results of Chamkha [27]
0.0	- 1.70593247	- 1.7167	0.0	- 1.06885341	- 1.0699	0.16	- 1.70593247	- 1.7167
1.0	- 1.70593247	- 1.7167	1.0	- 1.70593247	- 1.7167	0.60	- 1.70593247	- 1.7167
2.0	- 1.70593247	- 1.7167	2.0	- 2.11920647	- 2.1193	1.00	- 1.70593247	- 1.7167
3.0	- 1.70593247	- 1.7167	3.0	- 2.43881304	- 2.4388	2.00	- 1.70593247	- 1.7167

Tables 1, 2 and 3 present the comparison of skin-friction, rate of heat and mass transfer coefficients for the various values of Grashof number for mass transfer, Heat absorption and Schmidt number with previous published results of Chamkha [27] in absence of angle of inclination and Jeffrey fluid. From these tables, It is observed that our present results are in good agreement with the published results of Chamkha [27] in limiting sense.

Table-3: Comparison of present Sherwood number results with the Sherwood number results of Chamkha [27] for different values of Grashof number for mass transfer, Heat absorption and Schmidt number

Gc	Present Sherwood number results	Sherwood number results of Chamkha [27]	ϕ	Present Sherwood number results	Sherwood number results of Chamkha [27]	Sc	Present Sherwood number results	Sherwood number results of Chamkha [27]
0.0	- 0.80975314	- 0.8098	0.0	- 0.80975314	- 0.8098	0.16	- 0.22315462	- 0.2231
1.0	- 0.80975314	- 0.8098	1.0	- 0.80975314	- 0.8098	0.60	- 0.80975314	- 0.8098
2.0	- 0.80975314	- 0.8098	2.0	- 0.80975314	- 0.8098	1.00	- 1.33960423	- 1.3425
3.0	- 0.80975314	- 0.8098	3.0	- 0.80975314	- 0.8098	2.00	- 2.66350862	- 2.6741

5. RESULTS AND DISCUSSION:

In this section, the influence of various physical parameters like Grashof number for heat transfer (Gr), Grashof number for mass transfer (Gc), Magnetic field parameter (M), Permeability parameter (K), Prandtl number (Pr), Schmidt number (Sc), Heat absorption parameter (S), Angle of inclination parameter (α) and Jeffrey fluid parameter (λ) on velocity, temperature and concentration profiles have been analyzed. In the present study following default parameter values are adopted for computations: $Pr = 0.71$, $M = 0.5$, $Gr = 1.0$, $Gc = 1.0$, $\lambda = 0.5$, $K = 0.5$, $Sc = 0.22$, $S = 0.5$, $n = 0.1$, $t = 1.0$, $A = 0.5$, $\varepsilon = 0.001$, $U_p = 0.5$ and $\alpha = 30^\circ$. All graphs therefore correspond to these values unless specifically indicated on the appropriate graph.

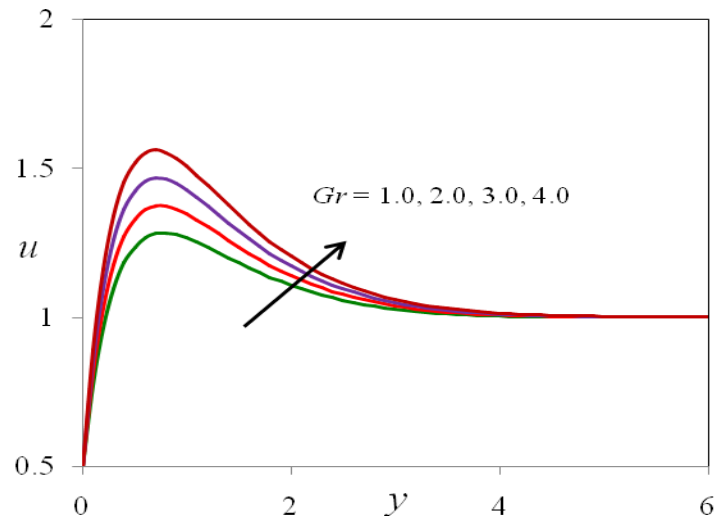


Fig. 2. Grashof number for heat transfer effect on velocity profiles

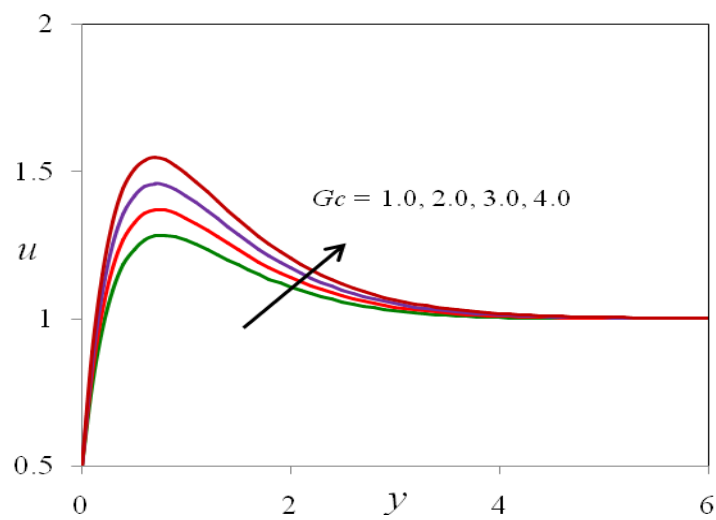


Fig. 3. Grashof number for mass transfer effect on velocity profiles

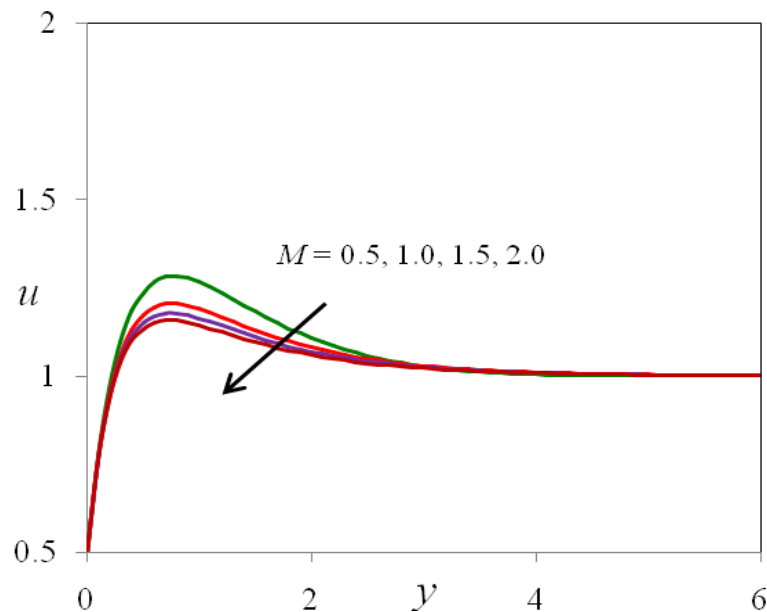


Fig. 4. Magnetic field parameter effect on velocity profiles

- ❖ Figs. 2 and 3 exhibit the effect of Grashof number for heat and mass transfer on the velocity profile with other parameters are fixed. The Grashof number for heat transfer signifies the relative effect of the thermal buoyancy force to the viscous hydrodynamic force in the boundary layer. As expected, it is observed that there is a rise in the velocity due to the enhancement of thermal buoyancy force. Also, as Gr increases, the peak values of the velocity increases rapidly near the porous plate and then decays smoothly to the free stream velocity. The Grashof number for mass transfer defines the ratio of the species buoyancy force to the viscous hydrodynamic force. As expected, the fluid velocity increases and the peak value is more distinctive due to increase in the species buoyancy force. The velocity distribution attains a distinctive maximum value in the vicinity of the plate and then decreases properly to approach the free stream value. It is noticed that the velocity increases with increasing values of the Grashof number for mass transfer.

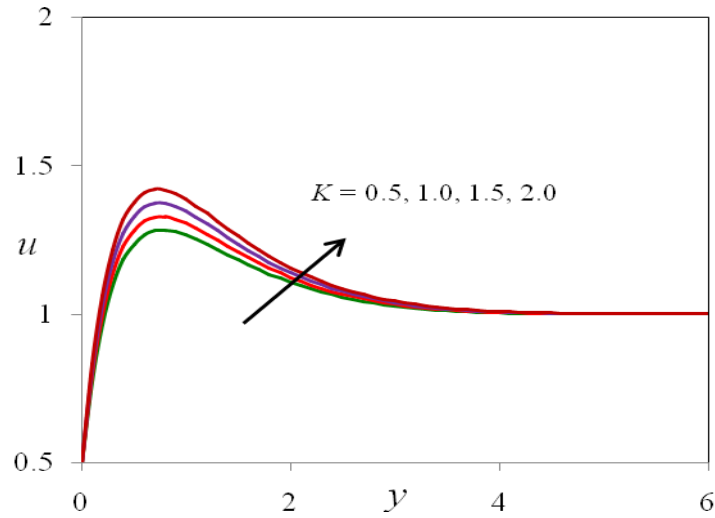


Fig. 5. Permeability parameter effect on velocity profiles

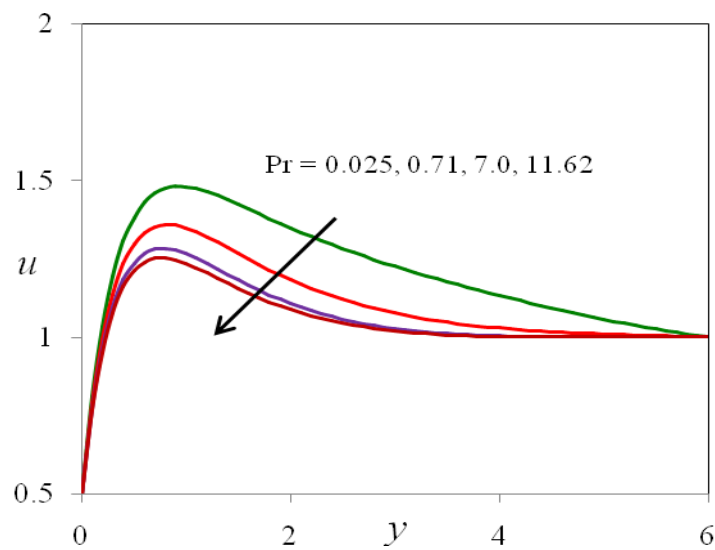


Fig. 6. Prandtl number effect on velocity profiles

- ❖ The effect of Magnetic field parameter (Hartmann number) on the velocity is shown in Fig. 4. The velocity decreases with an increase in the Hartmann number. It is because that the application of transverse magnetic field will result a resistive type force (Lorentz force) similar to drag force which tends to resist the fluid flow and thus reducing its velocity. Also, the boundary layer thickness decreases with an increase in the Hartmann number.
- ❖ Fig. 5 shows the effect of the permeability of the porous medium parameter on

the velocity distribution. As shown, the velocity is increasing with the increasing dimensionless porous medium parameter. Physically, this result can be achieved when the holes of the porous medium may be neglected.

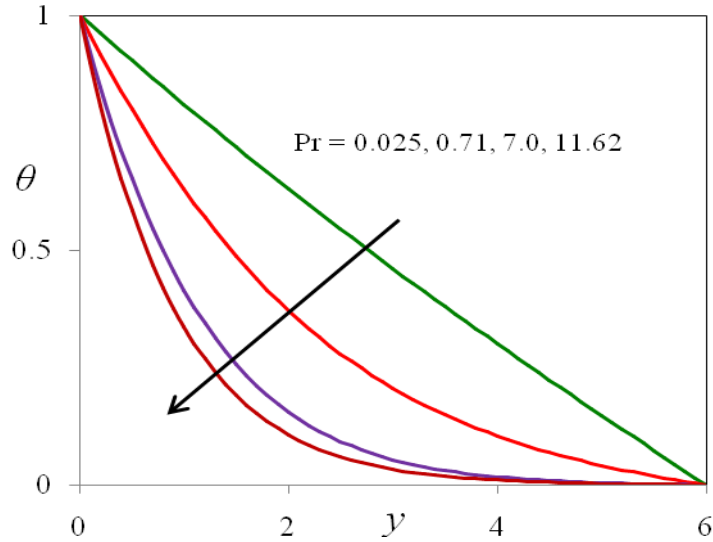


Fig. 7. Prandtl number effect on temperature profiles

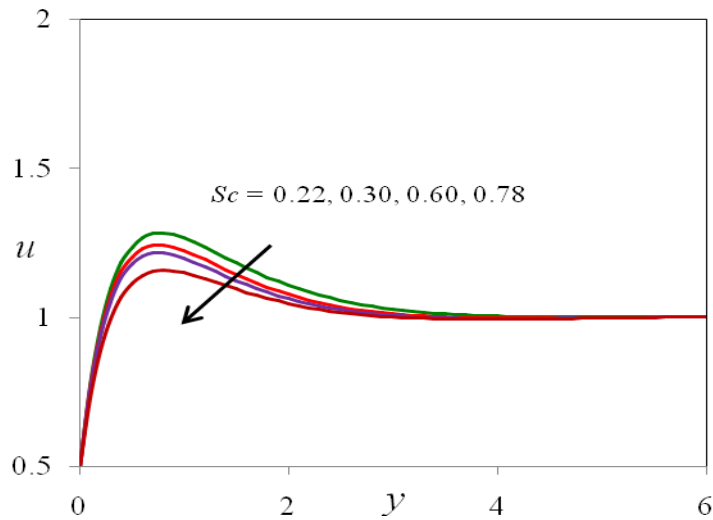


Fig. 8. Schmidt number effect on velocity profiles

- ❖ Fig. 6 depicts the effect of Prandtl number on velocity profiles in presence of foreign species such as Mercury ($Pr = 0.025$), Air ($Pr = 0.71$), Water ($Pr = 7.00$) and Methanol ($Pr = 11.62$). From this figure, we observed that , the velocity decreases with increasing of Prandtl number.

- ❖ In Fig. 7, we depict the effect of Prandtl number on the temperature field. It is observed that an increase in the Prandtl number leads to decrease in the temperature field. Also, temperature field falls more rapidly for water in comparison to air and the temperature curve is exactly linear for mercury, which is more sensible towards change in temperature. From this observation it is conclude that mercury is most effective for maintaining temperature differences and can be used efficiently in the laboratory. Air can replace mercury, the effectiveness of maintaining temperature changes are much less than mercury. However, air can be better and cheap replacement for industrial purpose. This is because, either increase of kinematic viscosity or decrease of thermal conductivity leads to increase in the value of Prandtl number. Hence temperature decreases with increasing of Prandtl number.
- ❖ Figs. 8 and 9 display the effects of the Schmidt number Sc on the velocity and concentration profiles at $t = 1$, respectively. As the Schmidt number increases, the concentration decreases. This causes the concentration buoyancy effects to decrease yielding a reduction in the fluid velocity. The reductions in the velocity and concentration profiles are accompanied by simultaneous reductions in the velocity and concentration boundary layers. These behaviours are clearly shown in Figs. 8 and 9.

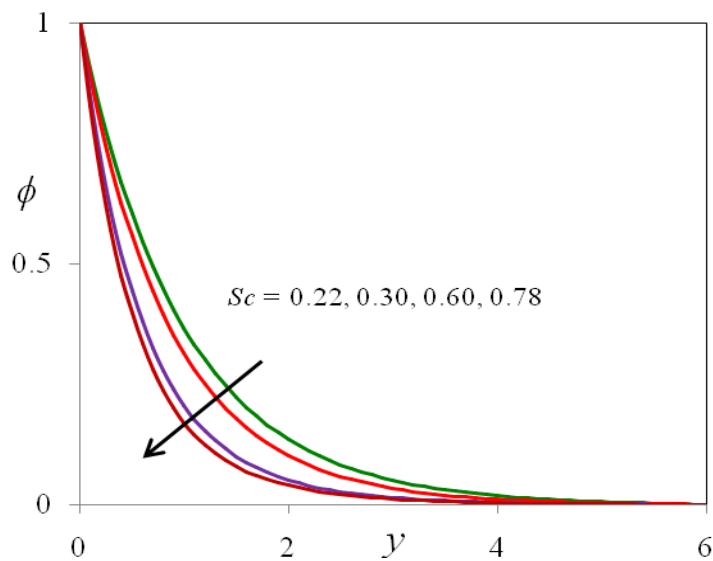


Fig. 9. Schmidt number effect on concentration profiles

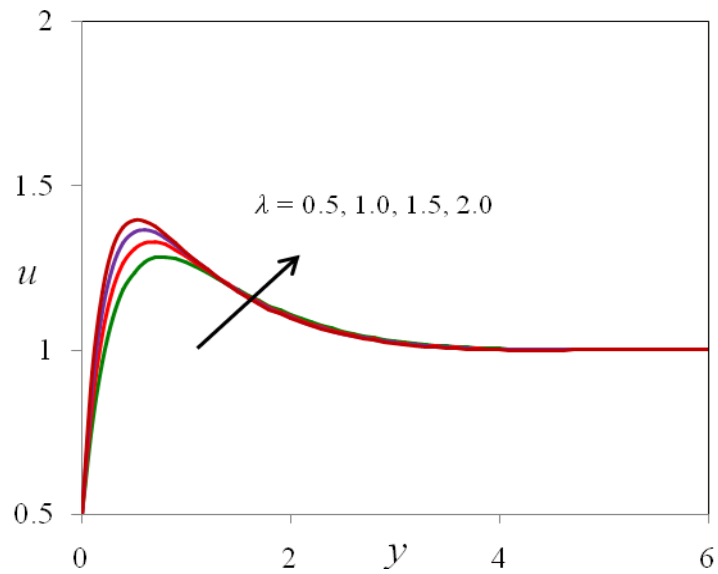


Fig. 10. Jeffrey fluid parameter effect on velocity profiles

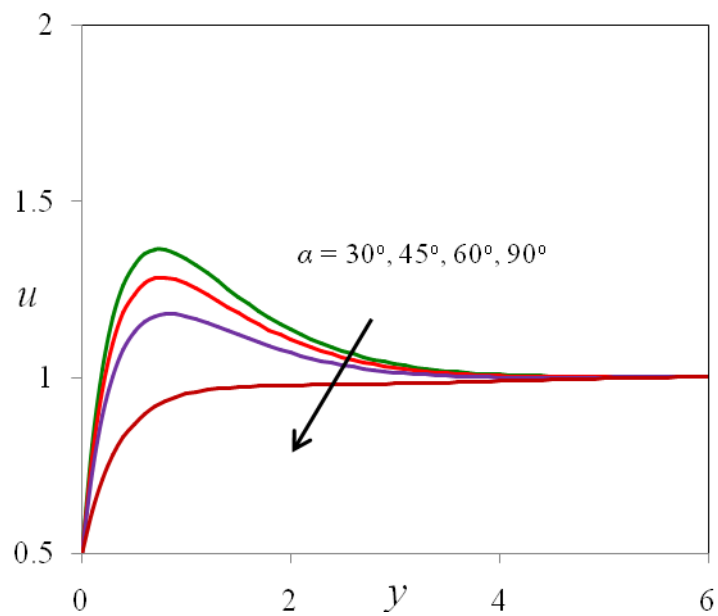


Fig. 11. Angle of inclination parameter effect on velocity profiles

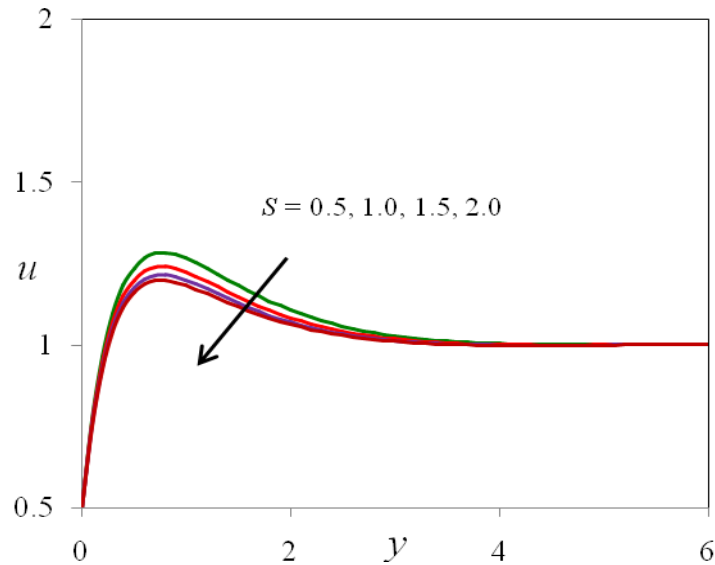


Fig. 12. Heat absorption parameter effect on velocity profiles

- ❖ The influence of Jeffrey fluid parameter on velocity profiles is as shown in the Fig. 10. It is observed that velocity profiles increases as Jeffrey fluid parameter increases.
- ❖ Fig. 11 demonstrates the influence of angle of inclination parameter on velocity profiles. From this figure, we observed that the velocity profiles is decreasing with increasing values of angle of inclination parameter.
- ❖ Figs. 12 and 13 illustrate the influence of the heat absorption coefficient S on the velocity and temperature profiles at $t = 1.0$, respectively. Physically speaking, the presence of heat absorption (thermal sink) effects has the tendency to reduce the fluid temperature. This causes the thermal buoyancy effects to decrease resulting in a net reduction in the fluid velocity. These behaviours are clearly obvious from Figs. 12 and 13 in which both the velocity and temperature distributions decrease as S increases. It is also observed that both the hydrodynamic (velocity) and the thermal (temperature) boundary layers decrease as the heat absorption effects increase.

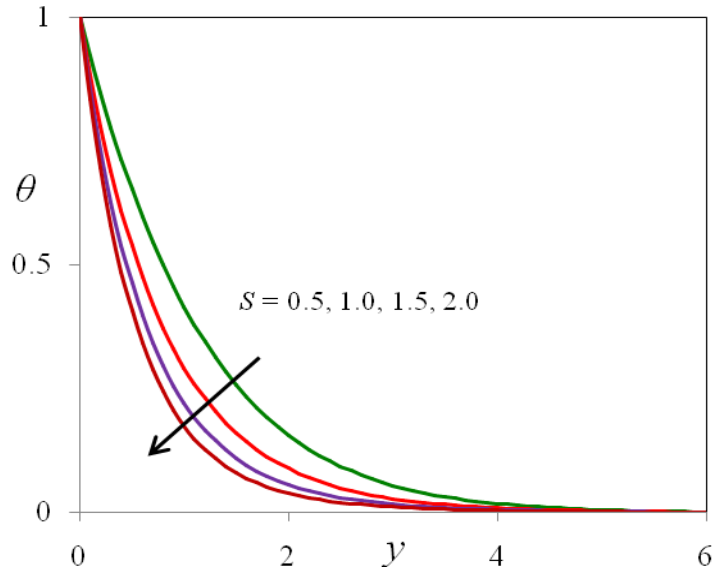


Fig. 13. Heat absorption parameter effect on temperature profiles

- ❖ The effects of various engineering governing parameters Grashof number for heat transfer, Magnetic field parameter, Permeability parameter, Prandtl number, Angle of inclination parameter, Jeffrey fluid parameter and time on the skin-friction coefficient is shown in table 4. It is observed that as the Grashof number for heat transfer or Permeability parameter or Jeffrey fluid parameter or time increases the skin-friction coefficient increases. It is found that as the Magnetic field parameter or Prandtl number or Angle of inclination parameter increases the skin-friction coefficient decreases.

Table-4: Skin-friction values for different values of $Gr, M, K, Pr, \alpha, \lambda$ and t

Gr	M	K	Pr	α	λ	t	τ
1.0	0.5	0.5	0.71	30°	0.5	1.0	3.24036417
2.0	0.5	0.5	0.71	30°	0.5	1.0	3.26248862
1.0	1.0	0.5	0.71	30°	0.5	1.0	3.17136654
1.0	0.5	1.0	0.71	30°	0.5	1.0	3.26554821
1.0	0.5	0.5	7.00	30°	0.5	1.0	3.19244783
1.0	0.5	0.5	0.71	45°	0.5	1.0	3.20477853
1.0	0.5	0.5	0.71	30°	1.0	1.0	3.25933461
1.0	0.5	0.5	0.71	30°	0.5	2.0	3.27631428

6. CONCLUSIONS:

The problem of influence of heat absorption on free convective of a magnetohydrodynamic Jeffrey fluid flow and over a vertically inclined plate in the presence of heat and mass transfer has been analyzed. The fundamental coupled partial differential equations were solved by applying finite difference method. The numerical results were obtained and compared with previously reported cases available in the literature and they were found to be in good agreement. Graphical results for various parametric conditions were presented and discussed for different values. From the present calculations, we may arrive at the following conclusions.

1. The magnetic field parameter retards the velocity of the flow field at all points, due to the magnetic pull of the Lorentz force acting on the flow field.
2. An increase in Prandtl number leads to a decrease of both velocity and temperature profiles.
3. An increase in the Grashof number for heat and mass transfer leads to an increase in the velocity profiles.
4. Velocity profiles as well as the concentration profiles decrease with an increase in the Schmidt number.
5. Both the velocity and temperature profiles decrease with an increase in the heat absorption.
6. Velocity profiles increase with an increase in Jeffrey fluid parameter while it decreases with an increase in Angle of inclination parameter.
7. The skin-friction coefficient increases for rising values of Grashof number for heat and mass transfer, Jeffrey fluid parameter and time.
8. In the absence of Jeffrey fluid and Angle of inclination observation of the present study coincides with published work of Chamkha [27].

REFERENCES:

- [1] K. Vajravelu, A. Hadjinicolaou, Convective heat transfer in an electrically conducting fluid at a stretching surface with uniform free stream, *Int J Eng Sci*, 35 (1997), p. 1237.
- [2] Pop, T.Y. Na, A note on MHD flow over a stretching permeable surface, *Mech Res Commun*, 25 (1998), pp. 263-269.
- [3] H. Xu, S.J. Liao, I. Pop, Series solutions of unsteady three-dimensional MHD flow and heat transfer in the boundary layer over an impulsively stretching plate, *Eur J Mech B-Fluids*, 26 (2007), pp. 15-27.
- [4] Ishak, R. Nazar, I. Pop, Hydromagnetic flow and heat transfer adjacent to a stretching vertical sheet, *Heat Mass Transfer*, 44 (2008), p. 921.
- [5] Ishak, K. Jafar, R. Nazar, I. Pop, MHD stagnation point flow towards a

- stretching sheet, *Phys A*, 388 (2009), pp. 3377-3383.
- [6] R.V.M.S.S. Kiran Kumar, P. Durga Prasad, S.V.K. Varma, Analytical study of heat and mass transfer enhancement in free convection flow with chemical reaction and constant heat source in nanofluids, *Procedia Eng*, 127 (2015), pp. 978-985.
- [7] R.V.M.S.S. Kiran Kumar, P. Durga Prasad, S.V.K. Varma, Thermo-diffusion and chemical reaction effects on free convective heat and mass transfer flow of conducting nanofluid through porous medium in a rotating frame, *Global J Pure Appl Math*, 12 (2016), pp. 342-351.
- [8] B. Venkateswarlu, P.V. Satyanarayana, Chemical reaction and radiation absorption effects on the flow and heat transfer of a nanofluid in a rotating system, *J Appl Nano Sci*, 5 (2015), pp. 351-360.
- [9] M.A. Mansour, Radiation and free convection effects on the oscillating flow past a vertical plate, *Astrophys. Space Sci.*, 166 (2) (1990), pp. 269-275.
- [10] P. Ganesan, P. Loganathan, Radiation and mass transfer effects on flow of an incompressible viscous fluid past a moving vertical cylinder, *Int. J. Heat Mass Trans.*, 45 (21) (2002), pp. 4281- 4288.
- [11] I.U. Mbeledogu, A.R.C. Amakiri, A. Ogulu, Unsteady MHD free convection flow of a compressible fluid past a moving vertical plate in the presence of radiative heat transfer, *Int. J. Heat Mass Trans.*, 50 (9-10) (2007), pp. 326-331.
- [12] O.D. Makinde, Free convection flow with thermal radiation and mass transfer past a moving vertical porous plate, *Int. Commun. Heat Mass Trans.*, 32 (10) (2005), pp. 1411-1419.
- [13] M.A. Samad, M.M. Rahman, Thermal radiation interaction with unsteady MHD flow past a vertical porous plate immersed in a porous medium, *J. Naval Arch. Marine Eng.*, 3 (1) (2006), pp. 7-14.
- [14] A. Orhan, K. Ahmet, Radiation effect on MHD mixed convection flow about a permeable vertical plate, *Heat Mass Transf.*, 2008 (2008).
- [15] N.R. Prasad, N.B. Reddy, R. Muthucumaraswamy, Transient radiation hydro-magnetic free convection flow past an impulsively started vertical plate with uniform heat and mass flux, *Theor. Appl. Mech.*, 33 (1) (2006), pp. 31-63.
- [16] H.S. Takhar, R.S.R. Gorla, V.M. Soundalgekar, Radiation effects on MHD free convection flow of a radiating gas past a semi infinite vertical plate, *Int. J. Num. Meth. Heat Fluid Flow*, 6 (2) (1996), pp. 77-83.
- [17] B. Gebhart, Y . Jaluria, R.L. Mahajan, *Buoyancy- Induced Flows and Transport*, Hemisphere Publishing Corporation, New York (1988).

- [18] M.M. Ali, T.S. Chen, B.F. Armaly, Natural convection-radiation interaction in boundary-layer flow over horizontal surfaces, *AIAA J.*, 22 (12) (1984), pp. 1797-1803.
- [19] M.A. Hossain, M.A. Alim, D.A.S. Rees, The effect of radiation on free convection from a porous vertical plate, *Int. J. Heat Mass Trans.*, 42 (1) (1999), pp. 181-191.
- [20] M.A. Hossain, D.A.S. Rees, I. Pop, Free convection-radiation interaction from an isothermal plate inclined at a small angle to the horizontal, *Acta Mech.*, 127 (1-4) (1998), pp. 63-73.
- [21] A.Y. Ghaly, Radiation effects on certain MHD free-convection flow, *Chaos, Solitons Fractals*, 13 (9) (2002), pp. 1843-1850.
- [22] R. Muthucumaraswamy, Janakiraman, MHD and radiation effects on moving isothermal vertical plate with variable mass diffusion, *Theor. Appl. Mech.*, 33 (1) (2006), pp. 17-29.
- [23] R. Muthucumaraswamy, Sivakumar, MHD flow past a parabolic flow past an infinite isothermal vertical plate in the presence of thermal radiation and chemical reaction, *Int. J. Appl. Mech. Eng.*, 21 (1) (2016), pp. 95-105.
- [24] N. Ahmed, M. Dutta, Analytical analysis of MHD transient flow past a suddenly started infinite vertical plate with thermal radiation and ramped wall temperature, *J. Heat Trans. (ASME)*, 136 (2014), pp. 041703-1-041703-8.
- [25] N. Ahmed, Soret and radiation effects on transient MHD free convection from an impulsively started infinite vertical plate, *J. Heat Trans. (ASME)*, 134 (2012), pp. 062701-1-062701-9.
- [26] R. Muthucumaraswamy, N. Dhanasekar, G.E. Prasad, Rotation effects on unsteady flow past an accelerated isothermal vertical plate with variable mass transfer in the presence of chemical reaction of first order, *J. Appl. Fluid Mech.*, 6 (4) (2013), pp. 485-490.
- [27] A. J. Chamkha, Unsteady MHD convective heat and mass transfer past a semi-infinite vertical permeable moving plate with heat absorption, *Int. J. Eng. Science*, 42 (2004), 217-230.
- [28] R. Srinivasa Raju, Combined influence of thermal diffusion and diffusion thermo on unsteady hydromagnetic free convective fluid flow past an infinite vertical porous plate in presence of chemical reaction, *Journal of the Institution of Engineers: Series C*, Vol. 97, Issue 4, pp. 505 – 515, 2016.
- [29] R. Srinivasa Raju, G. Jithender Reddy, J. Anand Rao, M. M. Rashidi, Rama Subba Reddy Gorla, Analytical and Numerical Study of Unsteady MHD Free Convection Flow over an Exponentially Moving Vertical Plate With Heat

- Absorption, *International Journal of Thermal Sciences*, Vol. 107, pp. 303 – 315, 2016.
- [30] R. Srinivasa Raju, B. Mahesh Reddy, M. M. Rashidi, Rama Subba Reddy Gorla, Application of Finite Element Method to Unsteady MHD Free Convection Flow Past a Vertically Inclined Porous Plate Including Thermal Diffusion And Diffusion Thermo Effects, *Journal of Porous Media*, Vol. 19, Issue. 8, pp. 701 – 722, 2016.
- [31] R. Srinivasa Raju, G. Jitthender Reddy, J. Anand Rao, M. M. Rashidi, Thermal Diffusion and Diffusion Thermo Effects on an Unsteady Heat and Mass Transfer MHD Natural Convection Couette Flow Using FEM, *Journal of Computational Design and Engineering*, Vol. 3, Issue 4, pp. 349 – 362, 2016.
- [32] R. Srinivasa Raju, G. Aruna, N. V. Swamy Naidu, S. Vijay Kumar Varma, M. M. Rashidi, Chemically reacting fluid flow induced by an exponentially accelerated infinite vertical plate in a magnetic field and variable temperature via LTT and FEM, *Theoretical Applied Mechanics*, Vol. 43, Issue 1, pp. 49 – 83, 2016.
- [33] R. Srinivasa Raju, Numerical Treatment Of Casson Fluid Free Convection Flow Past An Infinite Vertical Plate Filled In Magnetic Field In Presence Of Angle Of Inclination And Thermal Radiation: A Finite Element Technique, *International Journal of Engineering and Applied Sciences*, Vol. 8, No. 4, pp. 119 – 133, 2016.
- [34] G. Jitthender Reddy, R. Srinivasa Raju, J. Anand Rao, Rama Subba Reddy Gorla, Unsteady MHD Couette Flow of Water at 40C in a Rotating System in Presence of Heat Transfer with Ramped Temperature via Finite Element Method, Accepted for publication in *International Journal of Applied Mechanics and Engineering*, Vol. 22, No. 1, pp. pp. 145 – 161, 2017.
- [35] Sturdza P. An aerodynamic design method for supersonic natural laminar flow aircraft Ph. D. thesis. California, USA: Dept. Aeronautics and Astronautics, Stanford University, 2003.

